Carbohydrate Polymers 108 (2014) 291–298

Contents lists available at ScienceDirect

Carbohydrate Polymers

journal homepage: www.elsevier.com/locate/carbpol

Green synthesis of colloid silver nanoparticles and resulting biodegradable starch/silver nanocomposites

Perrine Cheviron[a,b,c], Fabrice Gouanvé[a,b,c,*], Eliane Espuche[a,b,c,**]

[a] Université de Lyon, F-69003 Lyon, France
[b] Université Lyon 1, F-69622 Villeurbanne, France
[c] CNRS, UMR5223, Ingénierie des Matériaux Polymères, France

ARTICLE INFO

Article history:
Received 25 November 2013
Received in revised form 24 January 2014
Accepted 12 February 2014
Available online 28 February 2014

Keywords:
Silver
Nanoparticle
Biopolymer
Green chemistry
Starch
Morphology

ABSTRACT

Environmentally friendly silver nanocomposite films were prepared by an ex situ method consisting firstly in the preparation of colloidal silver dispersions and secondly in the dispersion of the as-prepared nanoparticles in a potato starch/glycerol matrix, keeping a green chemistry process all along the synthesis steps. In the first step concerned with the preparation of the colloidal silver dispersions, water, glucose and soluble starch were used as solvent, reducing agent and stabilizing agent, respectively. The influences of the glucose amount and reaction time were investigated on the size and size distribution of the silver nanoparticles. Two distinct silver nanoparticle populations in size (diameter around 5 nm size for the first one and from 20 to 50 nm for the second one) were distinguished and still highlighted in the potato starch/glycerol based nanocomposite films. It was remarkable that lower nanoparticle mean sizes were evidenced by both TEM and UV–vis analyses in the nanocomposites in comparison to the respective colloidal silver dispersions. A dispersion mechanism based on the potential interactions developed between the nanoparticles and the polymer matrix and on the polymer chain lengths was proposed to explain this morphology. These nanocomposite film series can be viewed as a promising candidate for many applications in antimicrobial packaging, biomedicines and sensors.

1. Introduction

Biodegradable polymers from renewable resources have attracted much attention in recent years (Averous, Faucaonnier, Moro, & Fringant; Peterson, 2000; Hartman, Albertsson, Söderqvist Lindblad, & Sjöberg, 2006; Petersson & Oksman, 2006). Renewable sources of polymeric materials offer an alternative for maintaining the sustainable development of economically and ecologically attractive technologies. Indeed, the complete biological degradability of these polymers can contribute to a reduction in the volume of garbage and the protection of the climate through the reduction of the carbon dioxide release. Thus, there is considerable interest in replacing some or even a large amount of synthetic polymers by biodegradable materials and in combining them with inorganic nanofillers to achieve designed functional properties. Metal nanoparticles incorporated polymers attracted great attention because of widened application scope (Clémenson, Léonard, Sage, David, & Espuche, 2008; Nesher, Marom, & Anvir, 2008; Nimrodh Ananth, Umapathy, Sophia, Mathavan, & Mangalaraj, 2011; Wang, Wu, & Zhu, 2002; White, Budarin, Moir, & Clark, 2011). Particularly, polymer–silver nanocomposites are promising functional materials in fields such as optical, magnetic, electronic and antimicrobial properties (Duan, Huang, Cui, Wang, & Lieber, 2001; Huang & Yang, 2004; Huang, Yuan, & Yang, 2004; Jin, Cao, Mirkin, Kelley, Schatz, & Zheng, 2001; Lahav, Gabriel, Shipway, & Willner, 1999; Narayanan & El-Sayed, 2005; Sanpui, Murugadoss, Prasad, Ghosh, & Chattopadhyay, 2008). Different routes to introduce silver nanoparticles into synthetic polymer matrices have been developed over the past few years (Akamatsu et al., 2000; Chen, Chen, Serizawa, & Akashi, 1998; Dirix, Bastiaansen, Caseri, & Smith, 1999; Heilmann & Werner, 1998). In the last decade, many efforts have been made in the incorporation of silver nanoparticles into biodegradable polymers for their potential application in biotechnology (Murugadoss & Chattopadhyay, 2008). Polysaccharide polymers, such as chitosan, alginate and starch are the most extensively used as host matrices (Bozanic et al., 2011;

* Corresponding author at: Université de Lyon, F-69003, Lyon, France. Tel.: +33 04 72 43 12 10.
** Corresponding author at: Université de Lyon, F-69003, Lyon, France. Tel.: +33 04 72 43 27 01.
E-mail addresses: fabrice.gouanve@univ-lyon1.fr (F. Gouanvé), eliane.espuche@univ-lyon1.fr (E. Espuche).

http://dx.doi.org/10.1016/j.carbpol.2014.02.059
0144-8617/

Brayner, Vaulay, Fievet, & Coradin, 2007; Djokovic, Krsmanovic, Bozanic, McPherson, & Van Tendeloo, 2009; Khan et al., 2013; Vigneshwaran, Nachane, Balasubramanya, & Varadarajan, 2006; Vimala, Murali Mohan, Samba Sivudu, Varaprasad, Ravindra, 2010; Wei, Sun, Qian, & Ye, 2009). The general method consists in the dispersion of already prepared colloidal nanoparticles (AgNPs) in the polymer matrix solution (Lim & Ast, 2001). This method is often referred to as the evaporation method since the polymer solvent is evaporated from the reaction mixture after AgNPs dispersion. In all cases, the performance level of the nanocomposites depends on the controlled distribution of the uniformly shaped and sized nanoparticles. Improved properties are generally obtained when small dispersed nanodomains are obtained (Wiley, Sun, & Xia, 2007). Therefore, the controllable synthesis of AgNPs is the first key challenge to achieve their better applied characteristics. Colloidal silver nanoparticles can be prepared by physical, biological and chemical methods. The chemical approach is mostly used and consists in the treatment of silver salts with a chemical reducing agent, such as hydrazine, ethylenediaminetetraacetic acid and above all sodium borohydride (Bright, Musick, & Natan, 1998; Evanoff & Chumanov, 2004; Merga, Wilson, Lynn, Milosavljevic, & Meisel, 2007; Wang, Efrima, & Regev, 1998). However, most of these reducing agents are considered as non-environmentally friendly component. Increasing awareness about the total elimination or at least the minimization of the generated waste has led researchers to focus on alternative synthesis routes. Recently, efforts have been made for developing green methods to prepare silver nanoparticles (Anastas & Warner, 1998; Huang & Yang, 2004; Raveendran, Fu, & Wallen, 2003). The preparation of AgNPs via a green chemistry process should be evaluated from three specific aspects: the choice of the solvent medium, the choice of a non-toxic reducing agent and finally the choice of environmental friendly materials for the stabilization of the silver nanoparticles. Water is generally used as the environmental friendly solvent. Saccharide molecules such as aldehyde are generally used for the reduction of silver ions. Monosaccharide like glucose, galactose and fructose and disaccharide like maltose, lactose have been reported to lead to AgNPs of controllable sizes (Panacek, Kvıtek, Prucek, Kolar, & Vecerova, 2006; Mehta, Chaudhary, & Gradzielski, 2010). Glucose is one of the most widely-used green reducing agent due to its chemical reaction rate which allows a compromise between the number of nuclei created and the rate of growth of the silver nanoparticles (Mehta et al., 2010; Panigrahi, Kundu, Ghosh, Nath, & Pal, 2004). Polyethylene glycol and polysaccharides such as starch, chitosan and heparin are reported to stabilize silver nanoparticles (Fanta, Kenar, Felker, & Byars, 2013; Shameli et al., 2012; Sharma, Yngard, & Lin, 2009). In some cases, polysaccharides serve as both reducing and capping agent (Huang & Yang, 2004). In a nanocomposite approach, the choice of the capping agent is crucial to allow a good incorporation and final dispersion of AgNPs in the polymer matrix.

Among all the studies related with silver nanoparticles, very few works have been concerned with the whole steps of the preparation of biodegradable silver/polymer nanocomposites from green process including the synthesis of colloidal silver nanoparticles, their incorporation in a biodegradable polymer matrix and finally the characterization of the obtained nanocomposites. In the present paper, the synthesis of colloidal silver nanoparticles via a green chemistry process is reported. Water, glucose and soluble starch have been used as solvent, reducing agent and stabilizing agent, respectively. A kinetic study of the AgNPs formation was performed as a function of the concentration of reducing agent. The synthesis process was studied by using complementary techniques and the size and size distribution of the AgNPs were characterized. Starch based nanocomposite films were then prepared from the synthesized silver nanoparticles and their morphology was characterized. It was shown that by the green chemistry approach used in this study, it was possible at first to prepare very small silver nanoparticles and then to keep a fine dispersion of these nanoparticles within the biodegradable polymer matrix. This is a promising item for further functional fields such as medical applications and packaging.

2. Experimental

2.1. Materials

For colloidal silver nanoparticles preparation, $AgNO_3$ (ACS reagent > 99.0%) was purchased from Aldrich and used as silver precursor. D(+)-Glucose from Merck was used as reducing agent and soluble starch, supplied from Aldrich, was introduced as nanoparticles stabilizer. For the nanocomposite films elaboration, native potato starch with a weight ratio of amylopectin to amylase equal to 77/23 was purchased from Sigma and glycerol (99% purity-supplied from Aldrich) was used as plasticizer. In all cases, distilled water was used as solvent.

2.2. Preparation of the colloidal silver nanoparticles

In a typical experiment, 85 mg of soluble starch was dissolved in 25 mL of distilled water at 85 °C for 30 min. 10 mL of a 6.10^{-2} M silver nitrate was added into 25 mL of hot aqueous solution of soluble starch under vigorous stirring away from light. Then 15 mL of a glucose solution (0.06 M or 0.12 M) was added into the reactive system, which was held at 85 ± 0.5 °C with 700 rpm stirring. A thermostated oil bath and a magnetic stirrer were used to maintain a constant temperature and constant stirring throughout the reaction process. The molar fractions of $AgNO_3$/glucose used were 1:0, 1:1.5 and 1:3. The obtained colloidal suspension was cooled down at room temperature after different reaction times (between 1 and 72 h) and characterized. To avoid any photochemical reactions, all colloidal dispersions were kept in a dark place.

2.3. Preparation of the nanocomposite films

The film preparation consisted of the dissolution of potato starch in the presence of glycerol (weight ratio 85:15) in distilled water at a concentration of 3 wt%. The solutions were heated to the gelatinization temperature (85 °C) and continuously stirred at this temperature for 3 h. Then, an appropriate amount of colloidal silver nanoparticles was added and further stirred for 2 min at room temperature. The obtained mixture was poured into polystyrene Petri dishes and water evaporation was carried out at ambient temperature away from light during at least four days. The theoretical silver nanoparticles content in the films was 2 wt% and was expressed with respect to the total matter content including glycerol. Neat matrices were prepared by using the same experimental conditions. In all cases, the films were conditioned in dark place at 25 °C between two aluminum sheets before characterization. The thickness of the films was approximately 60 μm ± 5 μm.

2.4. Characterization methods

Different techniques were used to obtain complementary information about the size and the morphology of the silver nanoparticles in the colloidal suspensions and in the nanocomposite films.

2.4.1. Ultraviolet–visible absorption spectroscopy (UV–vis)

To follow the formation of silver nanoparticles and to investigate the influence of the embedded silver nanoparticles in the matrix, Ultraviolet–visible (UV–vis) absorption studies were performed on the colloidal silver nanoparticle dispersions and on the

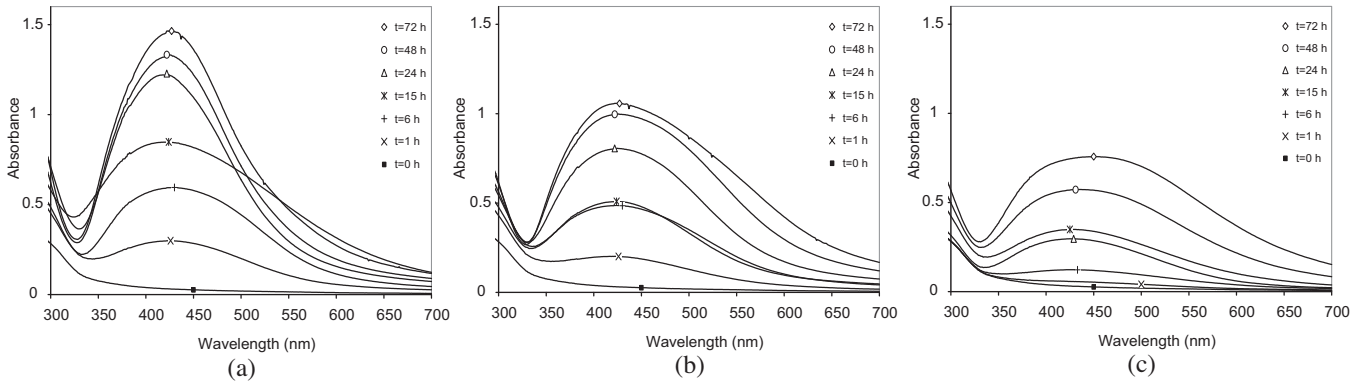

Fig. 1. UV–vis spectral evolution of silver nanoparticles using different $AgNO_3$/glucose molar ratio: (a) 1/3, (b) 1/1.5 and (c) 1/0.

different nanocomposite films with a Perkin Elmer Lambda 750 spectrophotometer in the wavelength range of 200–700 nm.

2.4.2. Transmission electron microscopy (TEM)

Size analysis of silver nanoparticles was carried out with a Philips CM120 electron microscope with an accelerating voltage of 120 kV. Two different methods were used to perform the colloidal silver nanoparticle dispersion analysis. In a first step a droplet of the aqueous dispersion was placed on Formwar coated grids. Then, in a second step, the colloidal droplets were dried either directly at room temperature for 10 min or after using a paper towel to obtain a thinner deposit. For the nanocomposite films analysis, samples were cut with a cryo-ultramicrotome at −90 °C with a Reicher Ultracut S instrument equipped with a diamond knife to obtain ultrathin sections of about 60 nm thicknesses. The samples were also placed on Formwar coated grids. For each analysis, low electron beam intensity was used and short time of exposure was performed to avoid any evolution of the samples during their exposure to the electron beam. The average diameter and size distribution of the nanoparticles were determined by the ImageJ Software based on the data of an average of 50–500 nanoparticles.

3. Results and discussion

3.1. Silver nanoparticles synthesis

Most of the studies based on green synthesis of silver nanoparticles using glucose and soluble starch as reducing agent and stabilizer, respectively considered a unique reaction time to prepare the nanoparticles. However, the chosen reaction time varied arbitrarily from 1 to 20 h depending on the authors (Aguilar-Mendez, San Martín-Martínez, Ortega-Arroyo, Cobián-Portillo, & Sánchez-Espíndola, 2011; Gao, Wei, Yan, & Xu, 2011; Raveendran et al., 2003; Shervani & Yamamoto, 2011; Singh, Sinha, & Mandal, 2009). In the present work, the reaction processes were studied for increasing reaction times in the range from 1 to 72 h at 85 °C. A series of reaction mixtures were prepared by keeping constant in each system the concentration of silver precursor (6.10^{-4} M) as well as the concentration of soluble starch used as stabilizer (0.17 wt%) and by varying the amount of reducing agent. The molar ratios of $AgNO_3$/glucose were 1:3 and 1:1.5 respectively. To investigate the role of the reducing agent in the reaction process, reaction mixtures were also prepared in the same conditions without glucose ($AgNO_3$/glucose molar ratio: 1:0). Different spectroscopic and microscopic techniques are routinely used to investigate the formation of silver nanoparticles (Anastas & Warner, 1998; Mehta et al., 2010; Raveendran et al., 2003; Shameli et al., 2012). UV–visible spectroscopy is one of the most important techniques to ascertain the formation and stability of silver nanoparticles in aqueous solution. The most characteristic evidence of silver nanoparticles formation is the surface plasmon resonance (SPR) bands observable in the 350–600 nm region (Burda, Chen, Narayanan, El-Sayed, 2005; Daniel & Astruc, 2004; Henglein, 1989). The shape of the spectra gives preliminary information about the size and the size distribution of the silver nanoparticles (Harada, Inada, & Nomura, 2009; Rafey, Shrivastavaa, Iqbal, & Khan, 2011). The UV–visible absorption spectra of silver nanoparticle dispersion at different reaction times for $AgNO_3$/glucose molar ratio of 1:3 and 1:1.5 are represented in Fig. 1a and b, respectively. In presence of the reducing agent, whatever the amount of glucose in the mixture, the intensity of the SPR peak increases with the increasing reaction time indicating a continued reduction of the Ag^+ ions. It can be also noticed that the absorption peak obtained for the reaction mixture prepared from $AgNO_3$/glucose molar ratio equal to 1:3 is characterized by a symmetrical shape whatever the reaction time. For the $AgNO_3$/glucose molar ratio of 1:1.5, the absorption peak has an asymmetric shape manifested by a widening toward long wavelengths. This widening at longer wavelengths indicates the presence of nanoparticle clusters (Huang et al., 1996; Patakfalvi, Viranyi, & Dekany, 2004). In order to evidence the role of glucose in the silver reduction process, the same experiments were also carried out without any glucose. The corresponding UV–vis absorption spectra at different reaction times are presented in Fig. 1c. The appearance of the SPR peak shows that the reduction of silver ions also takes place even if no glucose was added to the mixture. Thus, soluble starch has a double role: the one of a stabilizer and the one of a reducing agent. However, although the intensity of the SPR peak increases with the increase of the reaction time, the peak intensity remains lower compared to that one obtained for the mixture containing glucose, at the same reaction time. Moreover, the width of the peak also increases toward higher wavelengths as a function of the reaction time. The wavelength at the maximum of the absorbance (λ_{max}) as a function of the reaction time is represented in Fig. 2 for the different $AgNO_3$/glucose molar ratios. When glucose is added in the reaction mixture, λ_{max} is constant (422 ± 3 nm) and does not change as a function of the reaction time, independently of the glucose amount. In absence of glucose, the values of λ_{max} are also constant but slightly higher (427 ± 2 nm) than those obtained for the mixtures containing glucose for reaction times lower than 24 h. Up to this time, λ_{max} gradually increases as the reaction time increases. After 72 h of reaction, λ_{max} is around 450 nm. Fornasiero et al. have demonstrated that an increase in average size of the silver nanoparticles results in a shift of the absorption peak toward higher wavelengths (Fornasiero & Grieser, 1991). According to this work and to our results, an increase of the nanoparticle size should be expected. The rate of Ag^+ ion reduction was also determined for each $AgNO_3$/glucose ratio by examining the time dependence of maximal absorbance (A_{max}). The corresponding curves are

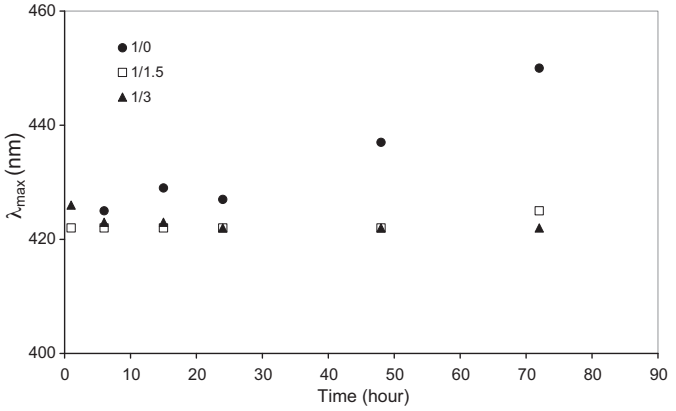

Fig. 2. Evolution of the wavelength at the maximal absorbance as a function of reaction time.

represented in Fig. 3. In presence of glucose, the curves clearly reveal that the A_{max} value rapidly increases during the initial period of the reaction and then reaches a constant value. The time to reach the plateau does not depend on the amount of reducing agent in the mixture. However, without glucose, the absorbance continuously increases as a function of the reaction time. The curves of absorbance time dependence represented in Fig. 3 were fitted by a first order rate equation according the following relationship:

$$A_t = A_\infty(1 - \exp(-k.t))$$

where A_t is the absorbance at time t, A_∞ the absorbance at very long time and k the first order-rate constant. For each system, the values of A_∞ and k are listed in Table 1 and the obtained theoretical curve is plotted in dotted line in Fig. 3. We can observe that the first order rate equation is convenient and well describes the experimental kinetics. For the different reaction media containing glucose, whatever the amount of glucose, the same value of k ($k = 1.5 \times 10^{-3}\ s^{-1}$) is obtained indicating a similar kinetic behavior of the reactions. The overall reaction mechanism is shown below:

$$2Ag^+ + H_2O + CH_2OH-(CHOH)_4 - (CHO) \rightarrow 2Ag + 2H^+ + CH_2OH-(CHOH)_4-(COOH)$$

However, in the absence of glucose in the mixture, the kinetic rate constant is 50 times lower. As explained by Gao et al. (2011), the aldehyde terminal of soluble starch can reduce silver nitrate while the presence of —OH and —O— groups of starch stabilize the silver nanoparticles. Furthermore, the value of A_∞ increases as the amount of glucose in the reaction mixture increases.

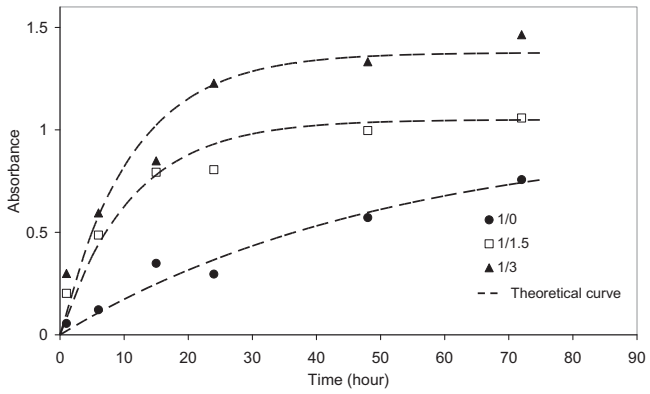

Fig. 3. Evolution of the maximal absorbance as a function of reaction time.

According to the classical crystallization theory, in presence of glucose, a large number of nuclei are formed and the obtained particle sizes are smaller and monodisperse. On the contrary, in the absence of glucose, a slow nucleation process is obtained leading to a small number of nuclei which grow and reach large polydisperse sizes (Khan, Al-Thabaiti, & Al-Nowaiser, 2012; Patakfalvi et al., 2004). So, for the molar ratios of $AgNO_3$/glucose under consideration in this study, we can conclude that glucose molecules tend to speed up the silver ions reduction and allow to limit the presence of silver nanoparticle clusters.

The sizes and morphology of synthesized silver nanoparticles were also imaged using Transmission Electron Microscope (TEM). Analyses were performed first by placing droplets of the undiluted dispersion on Formwar coated grids. Then, the grids were dried at room temperature for 10 min. Colloidal nanoparticle dispersion analyses were done for different reaction times (1, 6, 24, and 48 h) and for the three $AgNO_3$/glucose molar ratios (1:3, 1:1.5 and 1:0). Characteristic examples of the obtained images are shown in Fig. 4 for 1, 24 and 48 h of reaction. In a general point of view, the nanoparticles are isotropic and appear to be spherical. Two populations of nanoparticles can be distinguished. The first one is composed of larger nanoparticles that can be clearly distinguished due to their high enough phase contrast and the second one of very small nanoparticles (diameter less than 5 nm) which are characterized by a very low phase-contrast. In a first step, a quantitative analysis of the nanoparticles sizes was performed on the first highest size nanoparticles population. For all images, nanoparticle sizes were determined using the ImageJ Software based on the data of at least 50 measured nanoparticles for each picture. The histograms describing the dispersity in size distribution are also shown in Fig. 4. The obtained mean average nanoparticle size ($\overline{d}$) and associated standard deviation (σ) values are given in Table 1. The nanoparticle size $\overline{d}$ as a function of the reaction time for the different mixtures is also represented in Fig. 5. For the $AgNO_3$/glucose molar ratio equal to 1:3, the average particle size is around 20 nm and does not change as a function of time. More than 80% of the nanoparticles are in the size range from 10 to 30 nm. For long reaction time (48 h), only few particles over 30 nm are observed. Concerning $AgNO_3$/glucose molar ratio of 1:1.5, for reaction times lower than 6 h, the average size and the size distribution are equivalent to those obtained with the higher $AgNO_3$/glucose ratio (1:3). For time up to 6 h, the average size increases and is around 30 nm. More than 40% of the particles are bigger than 30 nm. Without glucose, the mean size and the size distribution are equivalent to those obtained in the presence of glucose but only for very short reaction times (less than 1 h of reaction). Then, the mean particle size increases as the reaction time increases. For 48 h of reaction, the mean particle size is around 47 nm and more than 60% of the nanoparticles are bigger than 30 nm. The quantitative data obtained from the TEM images are in good agreement with the previous qualitative conclusions drawn from the analysis of the UV–visible absorption spectra. However and as already discussed, very small-sized nanoparticles (less than 5 nm) could also co-exist with high-sized nanoparticles. It was difficult to perform quantitative analyses of these AgNPs due to their low phase contrast. In order to better observe this population of very small nanoparticles, the conditions used to prepare the samples for TEM observation were modified. Instead of drying directly the colloidal droplets at room temperature for 10 min, a paper towel was used to obtain thinner deposit and allow a better observation of the very small objects under the electron beam. A characteristic image of the colloidal solution obtained for 24 h of reaction time with a $AgNO_3$/glucose molar ratio of 1:3 is shown in Fig. 6. Numerous very small nanoparticles which are in a size range from 2 to 5 nm can be observed in addition to larger nanoparticles. However, the contrast remains

Table 1
Values of the parameters characterizing the first-order rate kinetic and corresponding mean silver nanoparticles size ($\bar{d}$) and associated standard deviation (σ) obtained from the colloidal dispersion.

$AgNO_3$/Glucose ratio	Kinetic		Nanoparticles size (nm)							
	A_∞	$k \times 10^3$ (s^{-1})	1 h		6 h		24 h		48 h	
			$\bar{d}$	σ	$\bar{d}$	σ	$\bar{d}$	σ	$\bar{d}$	σ
1/3	1.38	1.51	23	9	21	9	20	12	20	7
1/1.5	1.05	1.52	21	9	21	13	29	19	33	19
1/0	0.97	0.03	21	12	36	19	39	22	47	32

$\bar{d}$: mean nanoparticles size; σ:standard deviation.

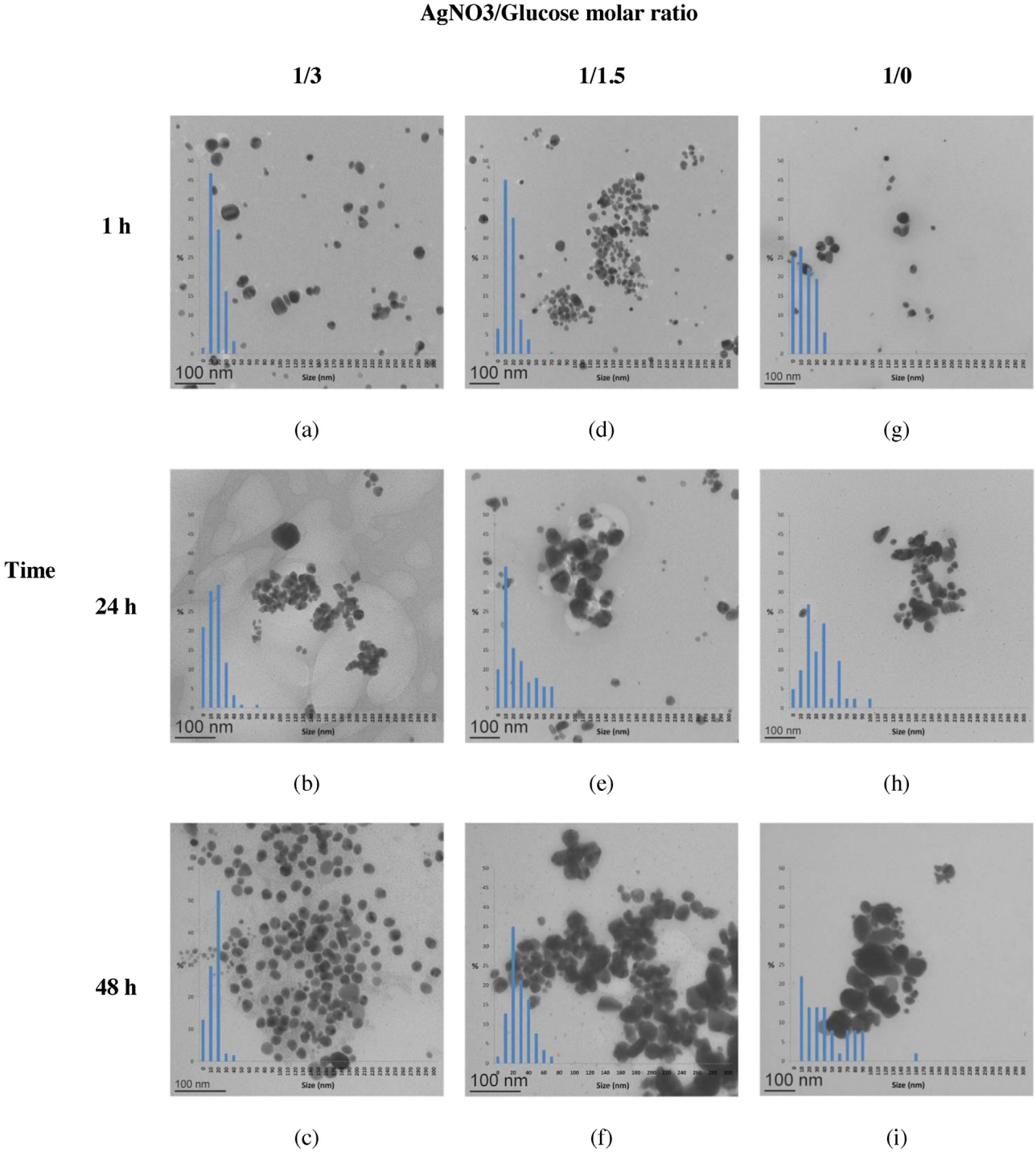

Fig. 4. Transmission electron micrographs for the colloidal dispersions for different reaction time and different $AgNO_3$/glucose molar ratio.

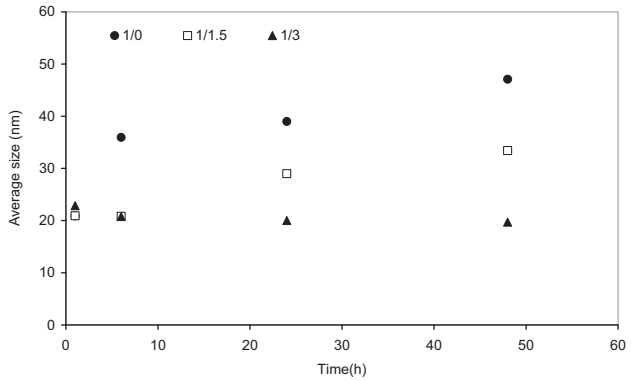

Fig. 5. Evolution of the average size of the silver nanoparticles as a function of reaction time.

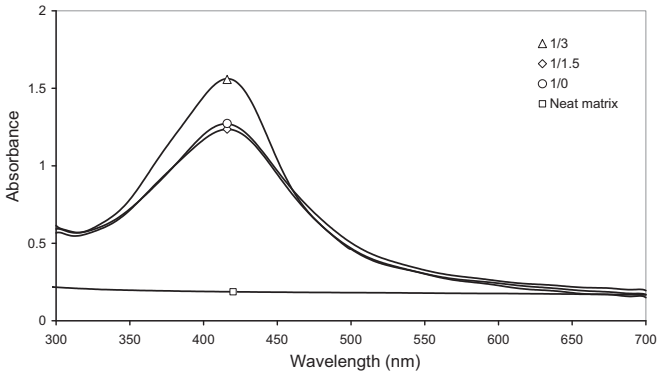

Fig. 7. UV–visible absorption spectra of nanocomposite films containing silver nanoparticles synthesized after 48 h of reaction time using different $AgNO_3$/glucose molar ratio and reference matrix.

too low to perform a quantitative analysis of this nanoparticle population.

3.2. Silver nanocomposite films

Nanocomposite films containing 2 wt% of silver were prepared by mixing an aqueous solution of potato starch and glycerol with the colloidal dispersions prepared from the three distinct $AgNO_3$/glucose molar ratios for 48 h of reaction respectively. According to UV analysis, for this reaction time, the reduction of silver ions is considered to be achieved when glucose is present in the mixture. The aqueous solutions containing potato starch, glycerol and AgNPs were cast and the water solvent was evaporated at room temperature away from light. The obtained films were handleable and not brittle. Furthermore, the colorless neat matrix film changed to light-orange color when silver nanoparticles were introduced. The UV–visible absorption spectra of the different nanocomposites and the neat matrix are presented in Fig. 7. The absorption values were normalized taking into account the real thickness of the films. Whatever the molar ratio of $AgNO_3$/glucose, the absorbance SPR peak confirms the presence of silver nanoparticles. The absorption peaks have a quite symmetrical shape and the wavelength of maximal absorbance is at 418 nm. It could also be noted that the widths of the absorption peaks of the different nanocomposites films are lower than those obtained for the associated colloidal dispersions. This difference of absorption peaks width and the shift of the absorption peak toward lower wavelength value can be explained by a change of organization of the silver nanoparticles when they are dispersed in water solvent and when they are embedded in the polymer matrix. Soluble starch chains which are used as capping agent can prevent more efficiently cluster formation of the silver nanoparticles when they are dispersed in the potato starch polymer matrix.

The dispersion of silver nanoparticles within the plasticized potato starch matrix was further analyzed using Transmission Electron Microscopy. The neat matrix was also imaged to be sure that neither the potato starch matrix nor the glycerol plasticizer creates any texturing which could alter the observation of the silver nanoparticles. Fig. 8a confirms that the plasticized neat matrix is homogenous. Fig. 8b–d shows TEM images of the nanocomposite films prepared from the silver colloidal dispersion synthesized from $AgNO_3$/glucose molar ratios of 1:3, 1:1.5 and 1:0, respectively. The nanoparticles are well distributed in the polymer matrix. Moreover, due to a sufficiently high phase contrast between the polymer matrix and the metal nanoparticles, it is possible this time to distinguish two different size populations in all nanocomposites and to perform a quantitative analysis of the nanoparticle sizes by Image J software, considering now all the nanoparticles. The first identified nanoparticle population corresponds to the silver nanoparticles of bigger size which were already identified in the colloidal aqueous silver dispersion. The sizes of these nanoparticles are in the same range order as that obtained for the respective colloidal dispersions. The second population which corresponds to the smallest nanoparticles represents 60% of the numbered nanoparticles in the nanocomposite films obtained from the silver colloidal dispersion synthesized in absence of glucose. It represents 90% of the numbered nanoparticles for the nanocomposites prepared

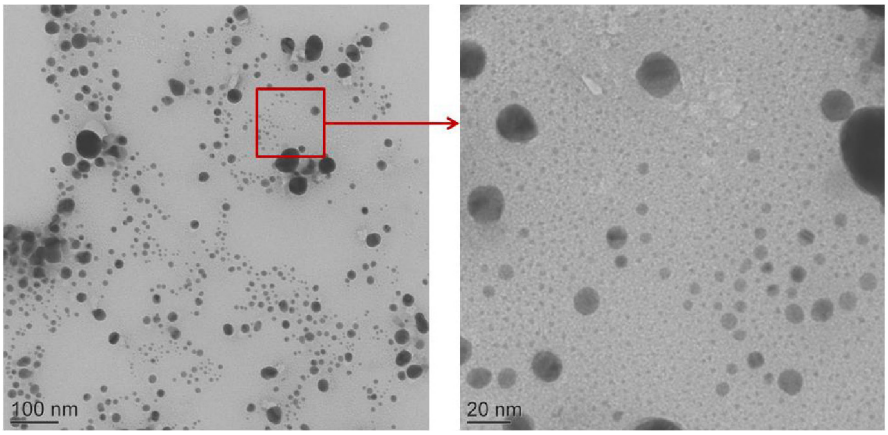

Fig. 6. Transmission electron micrographs for the colloidal dispersion for 24 h of reaction and $AgNO_3$/glucose molar ratio 1/3 using the towel paper method for the droplet drying.

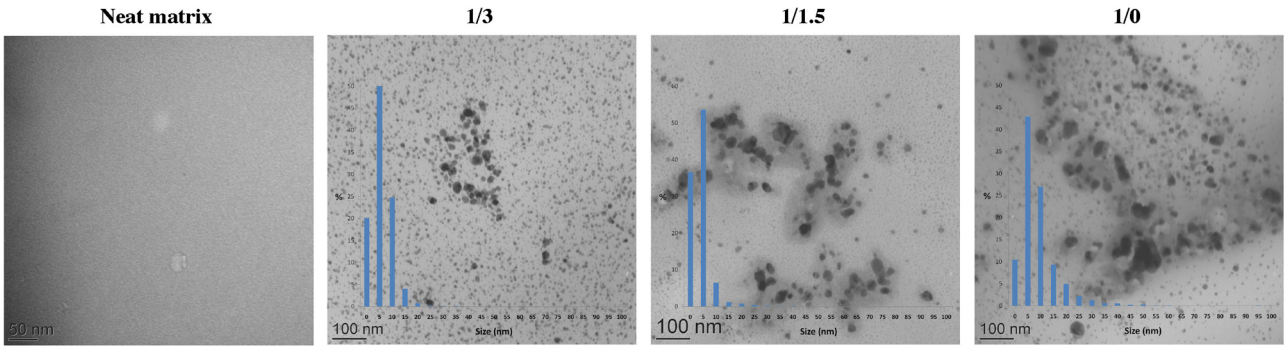

Fig. 8. Transmission electron micrographs for the nanocomposite films containing silver nanoparticles synthesized after 48 h of reaction time using different $AgNO_3$/glucose molar ratio: (a) neat matrix, (b) 1/3, (c) 1/1.5 and (d) 1/0.

from the silver colloidal dispersion synthesized in the presence of glucose. The average size of these particles is around 5 nm and it is similar whatever the amount of glucose used during the silver synthesis step. The observation of an important fraction of very small nanoparticles dispersed within the plasticized starch polymer matrix confirms firstly that very small sized nanoparticles could be synthesized via the green synthesis process that was proposed in this study and secondly that using plasticized potato starch as nanocomposite polymer matrix should prevent from aggregation phenomena. It was especially remarkable to evidence by both TEM observation and UV–visible analysis that the nanoparticle dispersion was improved in the polymer matrix in comparison to the colloidal dispersion. As discussed previously, the presence of soluble starch in the colloidal dispersion allows a better dispersion of the silver nanoparticles in the plasticized starch matrix due to their similar chemical structure and the high molar mass polymer chains of potato starch.

4. Conclusions

Colloidal silver nanoparticles were prepared at 85 °C via a green chemistry process by using water, glucose and soluble starch as solvent, reducing agent and stabilizing agent respectively. Reactions were carried out for $AgNO_3$/glucose molar ratios equal to 1:0, 1:1.5 and 1:3. Kinetics analyses of the silver nanoparticle formation were performed using ultraviolet-visible absorption spectroscopy and a first order kinetic was determined. When glucose was added in the reaction mixture, the reduction of silver ions was considered to be achieved after 48 h of reaction. At the $AgNO_3$/glucose levels of 1:3 and 1:1.5, the kinetic rate constant was similar ($k = 1.5\,10^{-3}\,s^{-1}$) whereas it was 50 times lower in absence of the reducing agent. Spherical silver nanoparticles were evidenced from TEM analysis. After 48 h of reaction, for a $AgNO_3$/glucose molar ratio equal to 1:3, a mean nanoparticles size of 20 nm was obtained whereas a larger mean size ($\bar{d} = 47$ nm) was determined in the absence of glucose in the reaction mixture. Then, nanocomposites were prepared via a solution/casting method by mixing the colloidal silver nanoparticle dispersions prepared for 48 h reaction time and a potato starch/glycerol solution. The silver content in the obtained films was fixed to 2 wt%. From TEM analysis, two distinct nanoparticle populations in size already suspected from colloidal dispersion analysis, were clearly highlighted. The first population corresponded to the silver nanoparticles which were analyzed in the colloidal dispersion, and it was characterized by a mean average particle size that was dependent on the glucose amount in the reaction mixture. The second population corresponded to very small nanoparticles whose size (around 5 nm) was independent on the amount of the reducing agent in the reaction mixture. The lower mean size of the nanoparticles evidenced by both TEM and UV–vis analyses, for the nanocomposites in comparison with the respective colloidal silver dispersions was mainly assigned to the interactions between the soluble starch and the plasticized starch matrix which favored the insertion of the starch polymer chain between the nanoparticles allowing then these long polymer chains to split-off the silver nanoparticles clusters during the film process formation.

From all our results, it could be concluded that by the green chemistry ex situ approach used in this study, it was possible at first to prepare very small silver nanoparticles and then to obtain a fine dispersion of these nanoparticles within the biodegradable starch/glycerol polymer matrix. These nanocomposite films series can be viewed as promising candidates for many applications in antimicrobial, biomedicines and sensors. Further work will be dealt with the preparation of biodegradable silver nanocomposite films directly from an in situ growing process of the silver nanoparticles via a green chemistry approach.

Acknowledgments

The authors are grateful to Ministry of Higher Education and Research for the financial support. They gratefully acknowledge Pierre Alcouffe and the Centre Technologique des Microstructures of University of Lyon 1 for TEM photomicrographs.

Appendix A. Supplementary data

Supplementary data associated with this article can be found, in the online version, at http://dx.doi.org/10.1016/j.carbpol.2014.02.059.

References

Aguilar-Mendez, M. A., San Martín-Martínez, E., Ortega-Arroyo, L., Cobián-Portillo, G., & Sánchez-Espíndola, E. (2011). Synthesis and characterization of silver nanoparticles: effect on phytopathogen Colletotrichum gloesporioides. *Journal of Nanoparticle Research*, *13*, 2525–2532.

Akamatsu, K., Takei, S., Mizuhata, M., Kajinami, A., Deki, S., Takeoka, S., et al. (2000). Preparation and characterization of polymer thin films containing silver and silver sulfide nanoparticles. *Thin Solid Films*, *359*, 55–60.

Anastas, P. T., & Warner, J. C. (1998). *Green chemistry: Theory and practice*. New York: Oxford University Press.

Averous, L., Fauconnier, N., Moro, L., & Fringant, C. (2000). Blends of thermoplastic starch and polyesteramide: Processing and properties. *Journal of Applied Polymer Science*, *76*, 1117–1128.

Bozanic, D. K., Djokovic, V., Dimitrijevic-Brankovic, S., Krsmanovic, R., McPherson, M., Nair, P. S., et al. (2011). Inhibition of microbial growth by silver–starch nanocomposite thin films. *Journal of Biomaterials Science*, *22*, 2343–2355.

Brayner, R., Vaulay, M. J., Fievet, F., & Coradin, T. (2007). Alginate-mediated growth of Co, Ni, and CoNi nanoparticles: Influence of the biopolymer structure. *Chemistry of Materials*, *19*, 1190–1198.

Bright, R. B., Musick, M. D., & Natan, M. J. (1998). Preparation and characterization of Ag colloid monolayers. *Langmuir*, *14*, 5695–5701.
Burda, C., Chen, X., Narayanan, R., & El-Sayed, M. A. (2005). Chemistry and properties of nanocrystals of different shapes. *Chemical Reviews*, *105*, 1025–1102.
Chen, C. W., Chen, M. Q., Serizawa, T., & Akashi, M. (1998). In-situ formation of silver nanoparticles on poly(N-isopropylacrylamide)-coated polystyrene microspheres. *Advanced Materials*, *10*, 1122–1126.
Clémenson, S., Léonard, D., Sage, D., David, L., & Espuche, E. (2008). Metal nanocomposite films prepared in situ from PVA and silver nitrate. Study of the nanostructuration process and morphology as a function of the in situ routes. *Journal of Polymer Science Part A: Polymer Chemistry*, *46*, 2062–2071.
Daniel, M. C., & Astruc, D. (2004). Gold nanoparticles: Assembly, supramolecular chemistry, quantum-size-related properties, and applications toward biology, catalysis, and nanotechnology. *Chemical Reviews*, *104*, 293–346.
Dirix, Y., Bastiaansen, C., Caseri, W., & Smith, P. (1999). Oriented pearl-necklace arrays of metallic nanoparticles in polymers: A new route toward polarization-dependent color filters. *Advanced Materials*, *11*, 223–227.
Djokovic, V., Krsmanovic, R., Bozanic, D. K., McPherson, M., & Van Tendeloo, G. (2009). Adsorption of sulphur onto surface of silver nanoparticles stabilized with sago starch biopolymer. *Colloid and Surface B: Biointerfaces*, *73*, 30–35.
Duan, X., Huang, Y., Cui, Y., Wang, J., & Lieber, C. M. (2001). Indium phosphine nanowires as building blocks for nanoscale electronic and optoelectronic devices. *Nature*, *409*, 66–69.
Evanoff, J. D., & Chumanov, G. J. (2004). Size-controlled synthesis of nanoparticles. 1. Silver-only aqueous suspensions via hydrogen reduction. *Journal of Physical Chemistry B*, *108*, 13948–13956.
Fanta, G. F., Kenar, J. A., Felker, F. C., & Byars, J. A. (2013). Preparation of starch-stabilized silver nanoparticles from amylose – Sodium palmitate inclusion complexes. *Carbohydrate Polymers*, *92*, 260–268.
Fornasiero, D., & Grieser, F. (1991). The kinetics of electrolyte induced aggregation of Carey Lea silver colloids. *Journal of Colloid and Interface Science*, *141*, 168–179.
Gao, X., Wei, L., Yan, H., & Xu, B. (2011). Green synthesis and characteristic of core–shell structure silver/starch nanoparticles. *Materials Letters*, *65*, 2963–2965.
Harada, M., Inada, Y., & Nomura, M. (2009). In situ time-resolved XAFS analysis of silver particle formation by photoreduction in polymer solutions. *Journal of Colloid and Interface Science*, *337*, 427–438.
Hartman, J., Albertsson, A. C., Söderqvist Lindblad, M., & Sjöberg, J. (2006). Oxygen barrier materials from renewable sources: Material properties of softwood hemicellulose-based films. *Journal of Applied Polymer Science*, *100*, 2985–2991.
Heilmann, A., & Werner, J. (1998). In situ observation of microstructural changes of embedded silver particles. *Thin Solid Films*, *317*, 21–26.
Henglein, A. (1989). Small-particle research – Physicochemical properties of extremely small colloidal metal and semiconductor particles. *Chemical Reviews*, *89*, 1861–1873.
Huang, H. H., Ni, X. P., Loy, G. L., Chew, C. H., Tan, K. L., Loh, F. C., et al. (1996). Photochemical formation of silver nanoparticles in poly(N-vinylpyrrolidone). *Langmuir*, *12*, 909–912.
Huang, H., & Yang, X. (2004). Synthesis of polysaccharide-stabilized gold and silver nanoparticles: A green method. *Carbohydrate Research*, *339*, 2627–2631.
Huang, H., Yuan, Q., & Yang, X. (2004). Preparation and characterization of metal–chitosan nanocomposites. *Colloids and Surfaces B: Biointerfaces*, *39*, 31–37.
Jin, R. C., Cao, Y. W., Mirkin, C. A., Kelley, K. L., Schatz, G. C., & Zheng, J. G. (2001). Photoinduced conversion of silver nanospheres to nanoprisms. *Science*, *294*, 1901–1903.
Khan, Z., Al-Thabaiti, S. A., & Al-Nowaiser, F. M. (2012). Kinetics of silver nanoparticle growth in aqueous polymer solutions. *Arabian Journal of Chemistry*, *5*, 453–459.
Khan, Z., Singh, T., Hussain, J. I., Obaid, A. Y., Al-Thabaiti, S. A., & El-Mossalamy, E. H. (2013). Starch-directed green synthesis, characterization and morphology of silver nanoparticles. *Colloids and Surfaces B: Biointerfaces*, *102*, 578–584.
Lahav, M., Gabriel, T., Shipway, A. N., & Willner, I. (1999). Assembly of a Zn(II)-porphyrin-bipyridinium dyad and Au-nanoparticle superstructures on conductive surfaces. *Journal of the American Chemical Society*, *121*, 258–259.
Lim, M. H., & Ast, D. G. (2001). Free-standing thin films containing hexagonally organized silver nanocrystals in a polymer matrix. *Advanced Materials*, *13*, 718–721.
Mehta, S. K., Chaudhary, S., & Gradzielski, M. (2010). Time dependence of nucleation and growth of silver nanoparticles generated by sugar reduction in micellar media. *Journal of Colloid and Interface Science*, *343*, 447–453.
Merga, G., Wilson, R., Lynn, G., Milosavljevic, B. H., & Meisel, D. (2007). Redox catalysis on Naked silver nanoparticles. *Journal of Physical Chemistry C*, *111*, 12220–12226.
Murugadoss, A., & Chattopadhyay, A. (2008). A 'green' chitosan–silver nanoparticles composite as a heterogeneous as well as micro-heterogeneous catalyst. *Nanotechnology*, *19*, 015603.
Narayanan, R., & El-Sayed, M. A. (2005). Catalysis with transition metal nanoparicles in colloidal solution: Nanoparticle shape dependence and stability. *Journal of Physical Chemistry B*, *109*, 12663–12676.
Nesher, G., Marom, G., & Anvir, D. (2008). Metal-polymer composites: Synthesis and characterization of polyaniline and other polymer at silver compositions. *Chemistry of Materials*, *20*, 4425–4432.
Nimrodh Ananth, A., Umapathy, S., Sophia, J., Mathavan, T., & Mangalaraj, D. (2011). On the optical and thermal properties of in situ/ex situ reduced Ag NP's/PVA composites and its role as a simple SPR-based protein sensor. *Applied Nanoscience*, *1*, 87–96.
Panacek, A., Kvıtek, L., Prucek, R., Kolar, M., & Vecerova, R. (2006). Silver colloid nanoparticles: Synthesis, characterization, and their antibacterial activity. *Journal of Physical Chemistry B*, *110*, 16248–16253.
Panigrahi, S., Kundu, S., Ghosh, S. K., Nath, S., & Pal, T. (2004). General method of synthesis for metal nanoparticles. *Journal of Nanoparticle Research*, *6*, 411–414.
Patakfalvi, R., Viranyi, Z., & Dekany, I. (2004). Kinetics of silver nanoparticle growth in aqueous polymer solutions. *Colloid & Polymer Science*, *283*, 299–305.
Petersson, L., & Oksman, K. (2006). Biopolymer based nanocomposites: Comparing layered silicates and microcrystalline cellulose as nanoreinforcement. *Composite Science and Technology*, *66*, 2187–2196.
Rafey, A., Shrivastavaa, K. B. L., Iqbal, S. A., & Khan, Z. (2011). Growth of Ag-nanoparticles using aspartic acid in aqueous solutions. *Journal of Colloid Interface Science*, *354*, 190–195.
Raveendran, P., Fu, J., & Wallen, S. L. (2003). Completely Green synthesis and stabilization of metal nanoparticles. *Journal of the American Chemical Society*, *125*, 13940–13941.
Sanpui, P., Murugadoss, A., Prasad, P. V. D., Ghosh, S. S., & Chattopadhyay, A. (2008). The antibacterial properties of a novel chitosan–Ag-nanoparticle composite. *International Journal of Food Microbiology*, *124*, 142–146.
Shameli, K., Bin Ahmad Jazayeri, S. D., Sedaghat, S., Shabanzadeh, P., Jahangirian, H., Mahdavi, M., et al. (2012). Synthesis and characterization of polyethylene glycol mediated silver nanoparticles by the green method. *International Journal of Molecular Sciences*, *13*, 6639–6650.
Sharma, V. K., Yngard, R. A., & Lin, Y. (2009). Silver nanoparticles: Green synthesis and their antimicrobial activities. *Advances in Colloid and Interface Science*, *145*, 83–96.
Shervani, Z., & Yamamoto, Y. (2011). Carbohydrate-directed synthesis of silver and gold nanoparticles: Effect of the structure of carbohydrates and reducing agents on the size and morphology of the composites. *Carbohydrate Research*, *346*, 651–658.
Singh, M., Sinha, I., & Mandal, R. K. (2009). Role of pH in the green synthesis of silver nanoparticles. *Materials Letters*, *63*, 425–427.
Vigneshwaran, N., Nachane, R. P., Balasubramanya, R. H., & Varadarajan, P. V. (2006). A novel one-pot 'green' synthesis of stable silver nanoparticles using soluble starch. *Carbohydrate Research*, *341*, 2012–2018.
Vimala, K., Murali Mohan, Y., Samba Sivudu, K., Varaprasad, K., & Ravindra, S. (2010). Fabrication of porous chitosan films impregnated with silver nanoparticles: A facile approach for superior antibacterial application. *Colloid and Surface B: Biointerfaces*, *76*, 248–258.
Wang, W., Efrima, S., & Regev, O. (1998). Directing oleate stabilized nanosized silver colloids into organic phases. *Langmuir*, *14*, 602–610.
Wang, P. H., Wu, Y. Z., & Zhu, Q. R. (2002). Polymer metal composite particles: Polymer core and metal shell. *Journal of Materials Science Letters*, *21*, 1825–1828.
Wei, D., Sun, W., Qian, W., & Ye, Y. (2009). The synthesis of chitosan-based silver nanoparticles and their antibacterial activity. *Carbohydrate Research*, *344*, 2375–2382.
White, R. J., Budarin, V. L., Moir, J. W. B., & Clark, J. H. (2011). A sweet killer: Mesoporous polysaccharide confined silver nanoparticles for antibacterial applications. *International Journal of Molecular Science*, *12*, 5782–5796.
Wiley, B., Sun, Y., & Xia, Y. (2007). Synthesis of silver nanostructures with controlled shapes and properties. *Accounts of Chemical Research*, *40*, 1067–1076.